Spectrochimica Acta Part A: Molecular and Biomolecular Spectroscopy 240 (2020) 118599

Contents lists available at ScienceDirect

Spectrochimica Acta Part A: Molecular and Biomolecular Spectroscopy

journal homepage: www.elsevier.com/locate/saa

Preparation of galactose oxidase functional phosphorescent quantum dots and detection of D-galactose

Jinzhi Lv *, Wenli Yang, Yanming Miao

Shanxi Normal University, Linfen 041004, PR China

ARTICLE INFO

Article history:
Received 18 April 2020
Received in revised form 4 June 2020
Accepted 6 June 2020
Available online 11 June 2020

Keywords:
Nano-biosensor
Galactose oxidase
Phosphorescence
D-galactose

ABSTRACT

Environmental friendly nano biosensor can improve the detection performance of traditional biomolecular sensors and have important application value in practical applications. In this study, a kind of room temperature phosphorescence (RTP) quantum dots (QDs) (GOX RTP QDs) nanobiosensor was prepared by mineralization at room temperature (25 °C), using galactose oxidase (GOX) as template, which improved the catalytic ability of traditional GOx to D-Galactose. The specific enzyme substrate reaction between GOx and D-Galactose and photoinduced electron transfer (Piet) were used to detect the RTP of D-galactose. The linear range of D-galactose detection is 0.02–0.8 mM, and the detection limit of the method is 0.008 mM. This method is based on the RTP property of QDs, which can effectively avoid the interference of background fluorescence of biological samples, and does not need complex sample pretreatment process. Therefore, this method is more suitable for the quantitative detection of D-Galactose in biological samples.

1. Introduction

The development of environmental friendly biosensor is an important part of modern biotechnology research. Green nano biosensor improves the detection performance of traditional biomolecular sensors due to its good biocompatibility, large specific surface area, many surface active centers, high catalytic efficiency and strong adsorption capacity, and is widely used in biological detection [1,2], clinical medicine diagnosis [3,4] and other industries.

Due to the characteristics of semiconductor QDs, such as high fluorescence quantum yield, light bleaching resistance, relatively narrow and symmetrical emission spectrum, wide range of continuous excitation spectrum and long light life, quantum dots have become the ideal material for the preparation of biosensors, and the biosensors have the advantages of higher sensitivity, better reliability, faster response speed and smaller volume. It has become an important content in the field of bioanalytical chemistry [5–14].

However, the preparation of QDs often needs to be synthesized in high temperature or more complex environment, and surface modification is needed to make them hydrophilic or biocompatible through connection, ligand exchange or other ligand coating. To further prepare biosensors, it also needs to be connected with proteins (antibodies, enzymes, etc.), DNA and other molecules to make QDs have biological target recognition performance, the process of functionalized QDs is not only complex and time-consuming, but also has poor stability, which limits its practical application. Therefore, directly using protein or DNA molecules as templates to synthesize QDs biosensors with high specificity and good stability is the first choice to solve the above problems.

Since proteins contain multiple residue groups like sulfydryl, amidogen, hydroxy and carboxyl and proteins match with QDs in size, proteins can be used as ligand to synthesize QDs, which is called the protein functionalized QDs [7–9]. Enzyme is a kind of protein with high specificity and catalytic activity to its substrate, and it is also the target part of many biosensors. Therefore, the QDs of enzyme functionalization should be an important part of the development of nano-biosensors, but the catalytic effect of enzyme depends on the integrity of the primary structure and spatial structure of enzyme molecules, if the enzyme molecules are denatured or subunit Depolymerization can result in the loss of enzyme activity. Therefore, how to synthesize QDs with enzyme as template under mild conditions becomes the key.

In addition, RTP QDs have many advantages compared with fluorescent QDs in term of optical properties. Firstly, RTP QDs (e.g. Mn-ZnS RTP QDs) has a longer triplet emission lifetime (ms level) and it can avoid interference of background fluorescence and emission light in complicated samples (e.g. biological fluids) [15,16]. Its detection selectivity is significantly higher due to the few occurrence of phosphorescence. Moreover, its Stroke shifts are relatively higher and the self-adsorption phenomenon is lighter, thus enabling to avoid interferences of excitation spectra. Secondly, RTP QDs require no deoxidant or inducer at detection, which decreases the complicated pre-processing [10,12,13,17]. Therefore, RTP QDs is more suitable for sensing target molecules in complex biological samples [8,11,12,18–23].

* Corresponding author.
E-mail address: lvjinzhi208@126.com (J. Lv).

https://doi.org/10.1016/j.saa.2020.118599
1386-1425/

Based on above reasons, a Mn-ZnS RTP QDs (GOX RTP QDs) nanobiosensor which uses GOX as template was prepared under a room temperature (25 °C). Besides, RTP detection of D-Galactose was achieved through specific recognition and decomposition of GOX to D-Galactose. The construction process is that: Zn^{2+} and Mn^{2+} react with GOX to generate biological mineral composites through biological mineralization. After S^{2-} is added in, GOX functionalized Mn-ZnS RTP QDs are generated (Fig. 1A). These RTP QDs are equipped with not only enzyme function of GOX, but also RTP properties as a kind of bi-functional nanomaterial. GOX can catalyze decomposition of D-Galactose into H_2O_2 and D-galacto-hexodialdose. H_2O_2 can quench RTP of QDs through electronic transfer. Based on this principle, a RTP biosensor for quantitative detection of D-Galactose was set up (Fig. 1B). Since this method is based on enzyme functions of GOX and RTP properties of QDs, this biosensor is characteristic of high specificity and can reduce interferences of background florescence and scattering light of biological samples effectively with respect to target detection. So it is more suitable for the quantitative detection of D-Galactose in biological samples.

2. Experimental

2.1. Materials and chemicals

Ultrapure water (18.2 MΩ·cm) was produced by a WaterPro ultrapure water system (Labconco, US). GOX (GOX > 70.0 U/mg) and D-Galactose were bought from Sangon (Shanghai) Co., Ltd. $Zn(Ac)_2{\cdot}2H_2O$, $Mn(Ac)_2{\cdot}4H_2O$, and $Na_2S{\cdot}9H_2O$ was purchased from Tianjin Kemiou Chemical Reagent Co., Ltd.

2.2. Apparatuses

RTP and Resonance Light Scattering (RLS) signals were tested by a Cary Eclipse fluorospectro photometer (Varian Company, USA). Material morphology was characterized on a Field Emission Transmission Electron Microscope (FEI Tecnai G2 F20 S-Twin Energy Dispersive Spectrometer: Oxford AZtec X-Max 80). Energy spectra were tested on the Super-X G2 EDS Detector (FEI Company). pH value was tested on a pH meter (Shanghai Leici, China). Ultraviolet/visible adsorption spectra (UV/Vis) were tested by a SPECORD 200 PLUS (Analytik Jena, Germany). XPS analysis was implemented on an X-ray Photoelectron Spectrometer (Thermo Fisher Scientific EscaLab 250Xi).

2.3. Synthesis of GOX RTP QDs

The synthesis of GOX RTP QDs: 100 μL GOX (1 mg/mL), 20 μL $MnAc_2$ (2.5 mM), 39 μL $ZnAc_2$ (50 mM) and 50 μL Tris-HCl solution (pH = 6.0, 0.1 M) were added into 259 μL secondary water, and then sealed up for 5 min reaction under 25 °C. Subsequently, 32 μL Na_2S (50 mM) was quickly added into the above reaction solution, and reacted for 20 min to obtain GOX RTP QDs.

2.4. Detection method

Test of D-Galactose: 0.5 mL Tris-HCl buffer solution (pH 7.8, 0.1 M) was added firstly. Secondly, 100 μL synthesized GOX RTP QDs solution was added and different volumes of D-Galactose solution (20 mM) was added, diluted to 5 mL and then oscillated evenly. RTP was tested 30 min later under the excitation wavelength of 305 nm.

2.5. Docking calculation between GOX and Zn^{2+}

GOX and Zn^{2+} were processed by autodocktools1.5.6, followed by distribution of atom types and generation of partial charges. Finally, they were stored in pdbqt format for molecular docking by using autodock vina.1.1.2. A total of 9 conformations were generated and the conformation with the best affinity was chosen as the final docking conformation. The interaction diagram of pymol1.7 was drawn. Vina docking parameters were set as the center coordinate of docking box: center_x = 13.935, center_y = 3.055, center_z = 19.862. The size of docking box was: size_x = 64, size_y = 56, size_z = 58. Besides, exhaustiveness = 32 and energy_range = 4. Other parameters were set in default. GOX structural information was collected from PDB database.

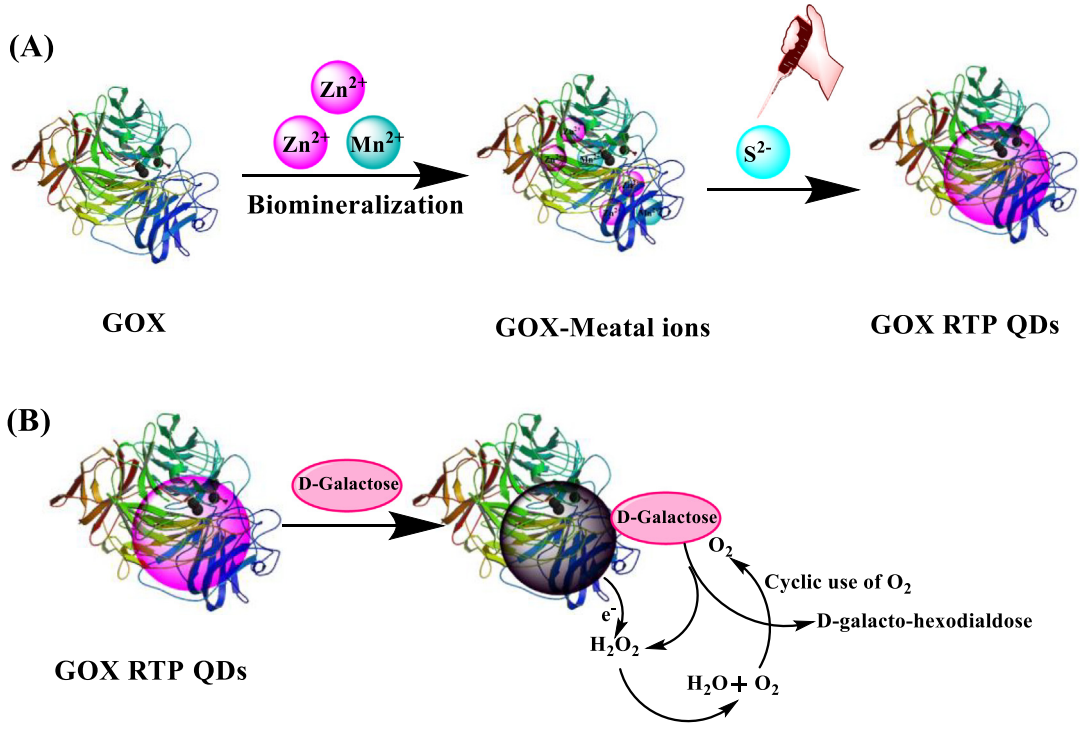

Fig. 1. (A) Synthesis process and diagram of GOX RTP QDs. (B) Detection of D-Galactose by GOX RTP QDs.

2.6. Docking calculation between GOX and D-galactose

D-Galactose 2D structure was drawn by ChemDraw and it was stored in cdx format. The cdx format was input by chem3D and the optimized results after MM2 force field was stored in pdb format for molecular docking. GOX and D-Galactose were processed by autodocktools1.5.6, followed by distribution of atom types and generation of partial charges. Finally, they were stored in pdbqt format for molecular docking by using AutoDock vina.1.1.2. A total of 9 conformations were generated and the conformation with the best affinity was chosen as the final docking conformation. The interaction diagram of pymol1.7 was drawn. Vina docking parameters were set as the center coordinate of docking box: center_x = 21.996, center_y = 11.236, center_z = 30.047. size of docking box: size_x = 20, size_y = 20, size_z = 20. exhaustiveness = 32, energy_range = 4. Other parameters were set as default.

2.7. Sample detection

In this study, urine was collected from healthy human body and was only diluted by 100 times. The standard dose of D-Galactose was set 0.1 mM, 0.2 mM and 0.3 mM, respectively. Sample detection steps are same as that in Section 2.4. The whole experiment repeated by 3 times.

3. Results and analysis

3.1. Optimization of synthesis conditions for GOX RTP QDs

In this study, GOX RTP QDs were synthesized directly under room temperature by using GOX as the template. Since concentration ratio, pH, temperature and aging time of reactant can influence optical properties of GOX RTP QDs significantly, preparation conditions of GOX RTP QDs were optimized.

With the increase of molar ratio between Mn^{2+} and (Mn^{2+}+Zn^{2+}), RTP intensity of GOX RTP QDs increases firstly and then decreases, and reaching the maximum at 2.5% (Fig. 2A). Luminescence after adulteration of Mn^{2+} is attributed to self-activation luminescence of ZnS and relevant luminescence related with Mn^{2+} center. With the increase of Mn^{2+} adulteration, Zn^{2+} vacancies are filled in by Mn^{2+} gradually. Accordingly, self-activation luminescence of ZnS weakens, whereas the relevant luminescence related with Mn^{2+} center increases. When the adulteration ratio is higher than 2.5%, the luminescence intensity will decline with the continuous growth of Mn^{2+} adulteration, thus resulting in concentration quenching. This is because excessive Mn^{2+} after Mn^{2+} vacancies are filled up by Mn^{2+} will be adsorbed onto the surface of GOX RTP QDs to capture electrons, thus resulting in RTP quenching [24].

With the increase of molar ratio of S^{2-}: (Mn^{2+} + Zn^{2+}), RTP intensity of GOX RTP QDs increases firstly and then decreases (Fig. 2B). RTP intensity reaches the maximum at 0.8 of molar ratio. Given a small molar ratio of S^{2-}: (Mn^{2+} + Zn^{2+}), it is difficult to form much effective luminescence centers of GOX RTP QDs. With the increase of S^{2-} proportion, the number of effective GOX RTP QDs also increases and RTP is enhanced gradually. With the continuous increase of S^{2-} proportion, excessive S^{2-} will be adsorbed onto the surface of GOX RTP QDs. These surface S^{2-} have relatively high reaction activity and are extremely instable. It is very easy to form luminescence quenching center with other atoms. Moreover, there are few S^{2-} vacancies in GOX RTP QDs due to excessive S^{2-} proportion. As a result, only few electron hole pairs are formed, which determines the low RTP intensity [11,20].

As shown in Fig. 2C, with the increase of GOX concentration, RTP intensity of GOX RTP QDs increases firstly and then decreases and reached the peak at 0.20 μM of GOX concentration. When the GOX concentration continues to increase, RTP intensity of GOX RTP QDs is decreased gradually. This might be because the proportion ratio of GOX in relative to Mn^{2+}, Zn^{2+} and S^{2-} is too higher when the GOX concentration is excessive, and QDs formed on GOX are decreased accordingly.

It can be seen from Fig. 2D that with the increase of pH, RTP intensity of GOX RTP QDs increases firstly and then decreases. The RTP intensity reaches the peak at pH 6.0, and then decreases with the further increase of pH. Due to equilibrium of various ions in the solution, the equilibrium among S^{2-}, H^{+} and amino acid residues will be broken under a relative small value of pH, thus decreasing the binding site between S^{2-} and amino acid residues in the solution. In this way, S on nanoparticle surface and amino acid residues will dissolve and separate from the equilibrium. Consequently, the nanocrystal surface will develop many defects, in which these vacancies become the nonradiative compound centers. Therefore, RTP intensity of GOX RTP QDs under small pH is relatively low. Because of the incomplete coordination of atoms on the surface of nanoparticles with large alkaline ratio, when pH is higher than 6.0, there are a lot of hanging bonds, so the strength of RTP decreases.

Based on above results, the optimal conditions for synthesis of GOX RTP QDs under room temperature is molar ratio of Mn^{2+}: (Mn^{2+}+-Zn^{2+}) = 2.5%, molar ratio of S^{2-}: (Mn^{2+}+Zn^{2+}) = 0.8, GOX concentration is 0.20 μM, and pH 6.0.

3.2. Characteristics of GOX RTP QDs

UV spectra of MPA covered Mn-ZnS QDs (curve a), GOX RTP QDs (curve b) and GOX (curve c) are shown in Fig. 3A. GOX RTP QDs shows a blue shift compared with MPA covered Mn-ZnS QDs. Since the absorption peak of GOX at 280 nm is smaller than the absorption peak wavelength of Mn-ZnS QDs, the superposition of GOX and Mn-ZnS QDs leads to the blue shift of the absorption peak of GOX RTP QDs. This also indicates that the RTP QDs which uses GOX as the template are synthesized.

According to Fig. 3B, the maximum excitation peak of GOX RTP QDs is 305 nm (curve a), and the maximum emission peak is 595 nm (curve b). This is because the RTP emission principle of GOX RTP QDs is that electrons on ZnS matrix are excited by the adsorbed excitation light and vacancies are captured by Mn^{2+}. Cavities and electrons are combined on Mn^{2+}, resulting in RTP of Mn^{2+} $^4T_1$-$^6A_1$ transition [11,25,26]. (hv_1 is the fluorescence caused by defects on ZnS surface and hv_2 is the phosphorescence caused by Mn^{2+} $^4T_1$-$^6A_1$ transition).

According to Fig. 3C and D, the average diameter of GOX RTP QDs is about 4.0 nm, and its Phosphorescence lifetime is 1.8 ms. The results of energy spectrum show that the synthesized GOX RTP QDs contain Mn, Zn and S. In this study, GOX RTP QDs and QDs without GOX coverage were analyzed by X-ray photoelectron spectroscopy (XPS). According to results, peaks of Zn (2p) of GOX RTP QDs occur at 1022.08 eV and 1044.89 eV (illustration in Fig. 3F), indicating Zn elements and GOX are combined. In addition, the peak at 1022.08 eV is a characteristic peak of ZnS, indicating that ZnS is formed by GOX RTP QDs.

Based on above results, GOX RTP QDs nanocomposites are prepared successfully in this study.

3.3. Detection of GOX RTP QDs used in D-galactose

Fig. 4A RTP shows that with the increase of D-Galactose concentration, the RTP intensity of GOX QDs is quenches gradually and regularly quenched, indicating that GOX RTP QDs can be used as RTP probe of D-Galactose. Under the optimal conditions, the ratio between RTP intensity quenching value of GOX RTP QDs and initial value of RTP ((RTP_0-RTP, △RTP)/RTP) and D-Galactose concentration conform to the equation (Fig. 4B):

$$1/(P_0-P) = 1/P_0 + K_{LB}/(P_0C_q)$$

where P_0 represents phosphorescence intensity of phosphor. P represents phosphorescence intensity of the system after phosphorescence quencher, C_q is the concentration of quencher. K_{LB} is the static quenching binding constant [27–29].

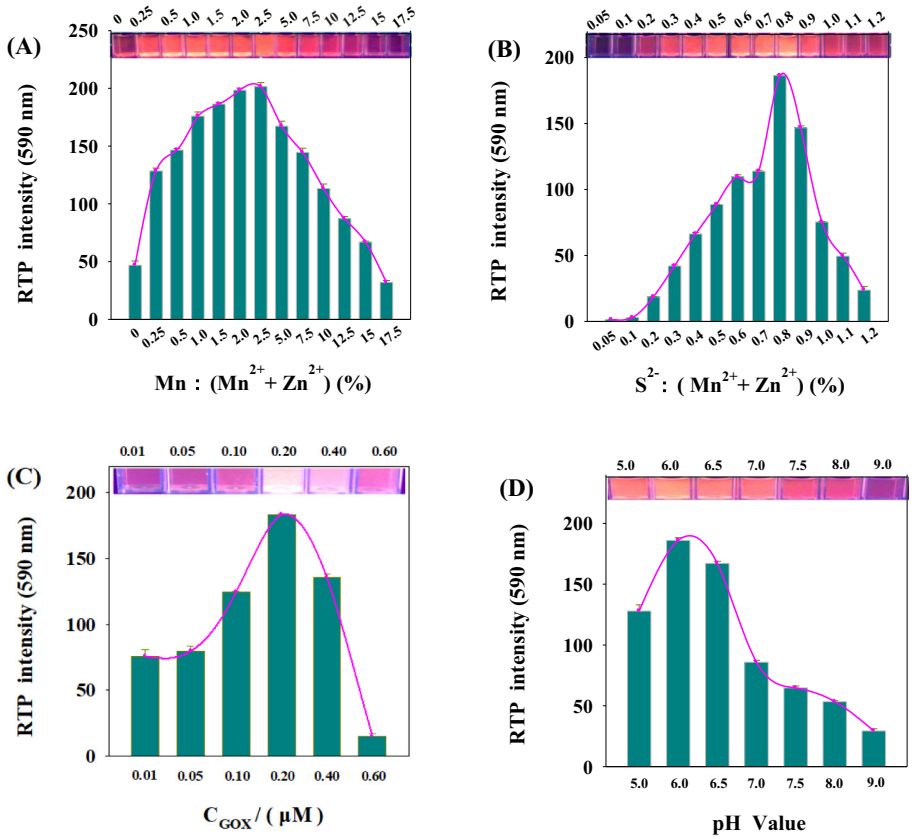

Fig. 2. (A) Relation between Mn^{2+}: (Mn^{2+}+Zn^{2+}) molar ratio and RTP intensity of GOX RTP QDs. (B) Relation between S^{2-}: (Mn^{2+}+Zn^{2+}) molar ratio and RTP intensity of GOX RTP QDs. (C) Relation between GOX concentration and RTP intensity of GOX RTP QDs. (D) Relation between pH and RTP intensity of GOX RTP QDs (λex = 305 nm, λem = 590 nm).

This RTP sensor has two linear ranges of D-Galactose detection, which are 0.02–0.1 mM and 0.1–0.8 mM, the detection limit of this method (3σ) is 0.008 mM.

The pH and temperature of solution can influence D-Galactose detection of GOX RTP QDs significantly. According to Fig. 4C, when pH is 7.8, the phosphorescence quenching rate (△RTP/RTP) reaches the maximum. Therefore, pH 7.8 was chosen as the optimal reaction condition. It can be seen from Fig. 4C that when the reaction temperature is 40 °C, △RTP/RTP reaches the maximum. Hence, 40 °C was chosen as the optimal reaction temperature.

Compared with other detection methods, The detection limit of this method was higher than Flow-injection [30], UV–visible Absorptiometry [31], Fluorescence [32], and lower than Electrochemistry method [33] (Table S1). Different from these methods, this method is based on RTP detection, which is not interfered by background fluorescence of biological samples, and does not need complex sample pretreatment process. So it is easy to operate. In addition, GOX RTP QDs in this study is not simply modified on the surface of QDs by linking, but directly synthesized GOX RTP QDs with GOX as the template. QDs and GOX are embedded with each other as a whole, which is more stable and easy to operate than the method of first preparing QDs and then linking enzyme molecules on its surface [34].

H_2O_2 is an excellent quencher for Mn-ZnS QDs [10]. Phosphorescence quenching of Mn-ZnS QDs by H_2O_2 is caused by electron transfer: the electrons on the conduction band of Mn-ZnS QDs are captured by H_2O_2, which inhibits the composition of electrons and holes produced by photoexcitation. Therefore, the detection principle of GOX RTP QDs system to D-Galactose is: GOX RTP QDs catalyze oxidization of D-Galactose to produce H_2O_2, while H_2O_2 quenches RTP of GOX RTP QDs. Meanwhile, H_2O_2 is reduced to O_2 and then O_2 participates in D-Galactose oxidization reaction catalyzed by GOX RTP QDs, finally forming the process of recycling O_2. This process is beneficial to the detection of D-Galactose by GOX RTP QDs, because O_2 is a common phosphorescence quencher. The recycling of O_2 in the process of catalytic oxidation of D-Galactose by GOX RTP QDs can avoid influences of O_2 on phosphorescence and increases sensing efficiency of GOX RTP QDs to D-Galactose.

3.4. Activity evaluation of GOX RTP QDs

In the presence of GOX, D-Galactose can be produced by oxidization of O_2 to generate D-Galactose acid and H_2O_2:

$$\text{D-Galactose} + O_2 + H_2O \longrightarrow \text{D-galacto-hexodialdose} + H_2O_2$$

The activity of GOX RTP QDs was also evaluated. Under the given enzyme activity, the production rate of H_2O_2 was proportional to D-Galactose concentration. Here, H_2O_2 is a phosphorescence quencher. Therefore, the degree of phosphorescence quenching is related to the activity of GOX enzyme directly. It can be seen from Fig. 5A that phosphorescence quenching basically reaches a platform in 30 min when the concentration of D-Galactose exceeds 0.6 mM. According to slope of enzyme reaction, Michaelis constant (K_m is used to characterize constant of enzyme-substrate interaction) of GOX is calculated. It can be calculated from the Lineweaver-Burke curve:

$$\frac{1}{v} = \frac{K_m}{V_{max}}\frac{1}{[S]} + \frac{1}{V_{max}}$$

According to the method proposed by Cao and Wu et al. [10,35], we calculated that the K_m value of GOx RTP QDs is 0.37 mM (Fig. 5B), while the K_m of GOX without fixed is 61 mM [36]. Since the smaller the Km value, the stronger the binding capacity of the enzyme to the substrate, so the affinity of GOx combined with QDs and D-Galactose is enhanced,

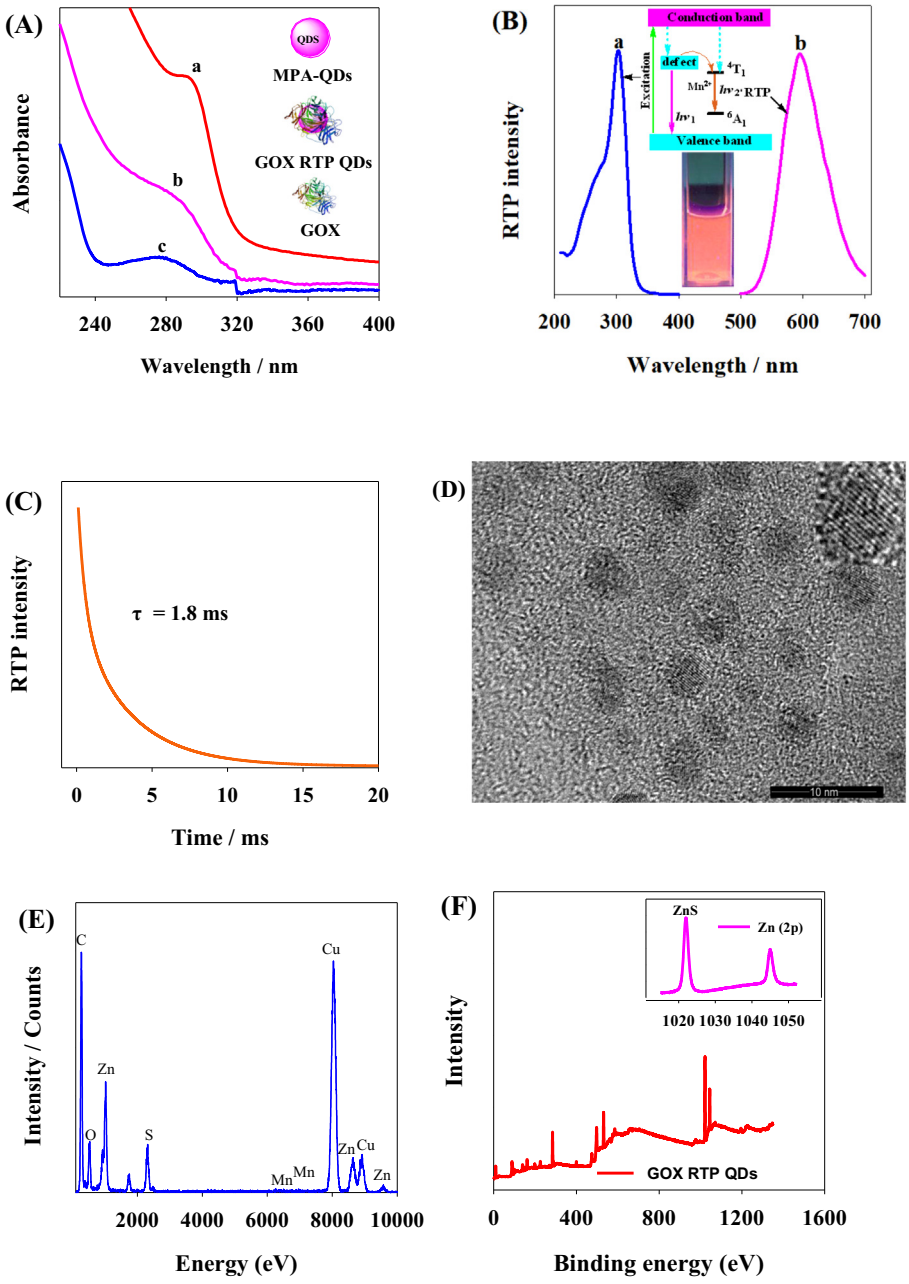

Fig. 3. UV spectra of MPA capped Mn-ZnS QDs (curve a), GOX RTP QDs (curve b) and GOX (curve c). (B) Maximum excitation peak (a) and maximum emission peak (b) of GOX RTP QDs. (C) phosphorescence lifetime of GOX RTP QDs. (D) TEM of GOX RTP QDs. (E) Energy diagram of GOX RTP QDs. (F) XPS diagram of GOX RTP QDs and the illustration is the XPS spectra of Zn.

and the enzyme activity is greatly improved. It is possible that QDs nanomaterials have large specific surface area and can combine with more GOx, which leads to the increase of catalytic activity.

3.5. Synthesis mechanism of GOX RTP QDs

In order to better study the formation process of GOX RTP QDs and the process of catalyzing D-Galactose, the docking calculation of the combination of GOX and Zn^{2+} as well as the combination of GOX and D-Galactose was carried out in this study (Table S2, Fig. 6). Select the docking structure with the most stable energy (Row 1 in Table S2) for analysis.

Since Zn^{2+} is the key ion to form QDs, docking between GOX and Zn^{2+} was calculated. Molecular docking reflects (Fig. 6A) that Zn^{2+} is bonded onto N-end structural domain of GOX. The bonding site is between a short section of α-helix and a section of loop structure. The affinity (binding free energy) is −2.0 kcal/mol. The interaction residues of Zn^{2+} are mainly Asp32, Thr37 and Glu142. Side chains of these three residues have relatively strong electronegativity. In particular, side chains of Asp and Glu are carboxyls which are negatively charged and can form a strong electrostatic interaction with positive charges of Zn^{2+}, and fix Zn^{2+}. The N-end structural domain of GOX is the main position of QDs.

In this study, docking calculation between GOX and D-Galactose molecules was carried out. The results show that D-Galactose binds to C-end with a large domain of GOX. The binding site was located in an active pocket with large flexibility, which is mainly surrounded by loop structure (Fig. 6B). The activity pocket has half strong hydrophilicity in and half strong hydrophobicity. Hydroxyls of D-Galactose are mainly towards the hydrophilic side, while carbon atoms are towards the hydrophobic side (Fig. 6C). The affinity (binding free energy) between D-Galactose and receptor protein is −4.9 kcal/mol.

D-Galactose binds to a Cu^{+} mediated catalytic site (Fig. 6D). Among them, Cu^{+} can bond with four residues (Tyr272, Tyr495, His496 and

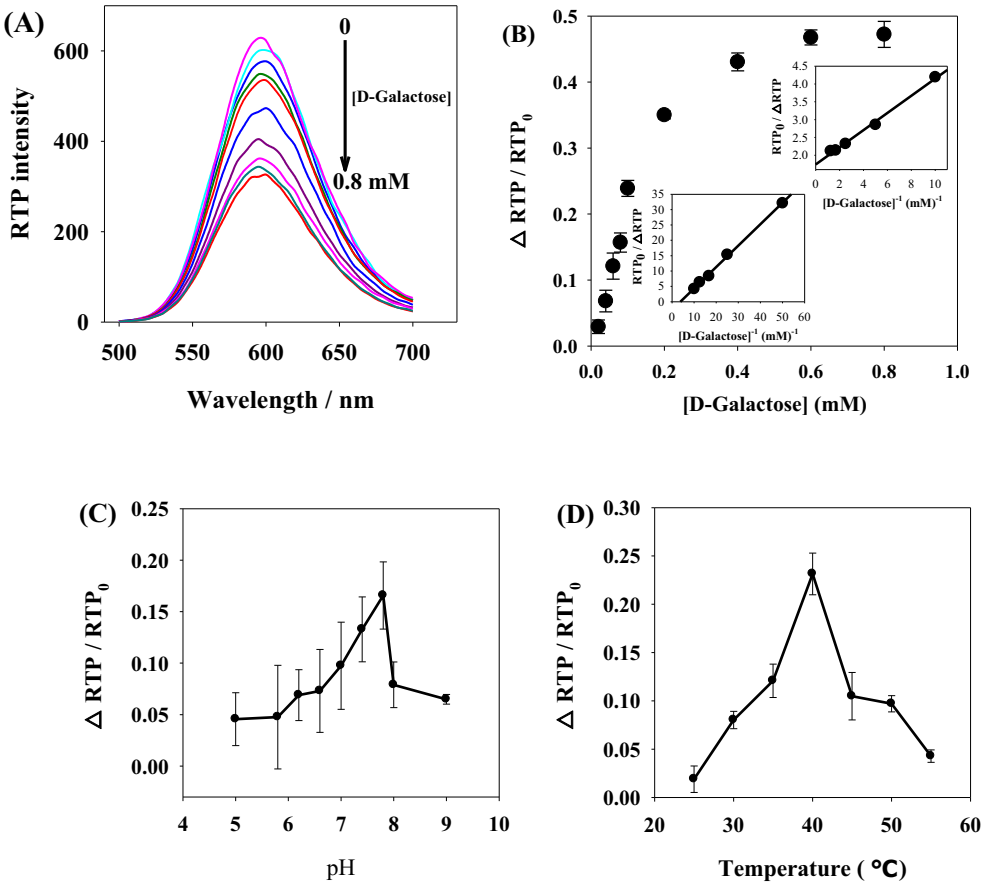

Fig. 4. (A) Variation spectra of RTP intensity of GOX RTP QDs with the increase of D-Galactose concentration; (B) Standard curve of D-Galactose detection based on GOX RTP QDs, Buffer, 10 mM Tris-HCl (pH 7.4) (C) Influences of pH on $\Delta RTP/RTP_0$ of D-Galactose + D-Galactose system. (D) Influences of temperature on $\Delta RTP/RTP_0$ of the D-Galactose + D-Galactose system.

His581) to form a complex structure. The distances between Cu^+ and key atoms of four residues are 2.1 Å, 2.9 Å, 2.0 Å and 2.1 Å, respectively. The complex structure is necessary for catalysis. In addition, Cys228 can form a covalent structure with Tyr272 through thioether bond. This structure can finally form Tyr radicals. The free radical is also vital to oxidization of catalyzed D-Galactose. Finally, the distance between hydroxyl oxygen on the 6C atom of D-Galactose and Cu^+ is 3.9 Å, which is relatively close to catalysis center and conducive to catalysis, that is, hydroxyl is oxidized.

According to molecular docking (Fig. 6E) the interaction residues with D-Galactose mainly include Phe194, Trp290, Tyr329, Arg330, Gln406, Pro463, Tyr495, etc. The hydroxyls of D-Galactose have hydrogen bonds with these residues. As shown in the dotted line, these hydrogen bonds play a key role in the stable binding and catalysis of D-Galactose.

Based on above results, the bonding positions of GOX and QDs are mainly at N end, and the bonding positions of GOX and D-Galactose are mainly at C end. Therefore, formation of GOX RTP QDs will not influence the binding between GOX and D-Galactose directly. However, the large specific surface area of QDs can carry much GOX, which can promote interaction between GOX and D-Galactose better on QDs surface. Therefore, GOX RTP QDs have high catalysis activity because of the abundant catalysis sites.

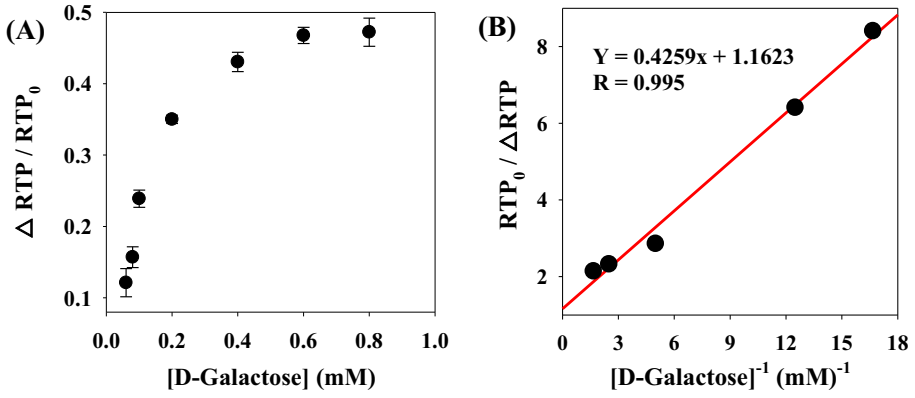

Fig. 5. (A) Variations of RTP intensity of GOX RTP QDs with the increase of D-Galactose concentration. (B) Lineweaver-Burke plots of the GOX RTP QDs/D-Galactose reaction.

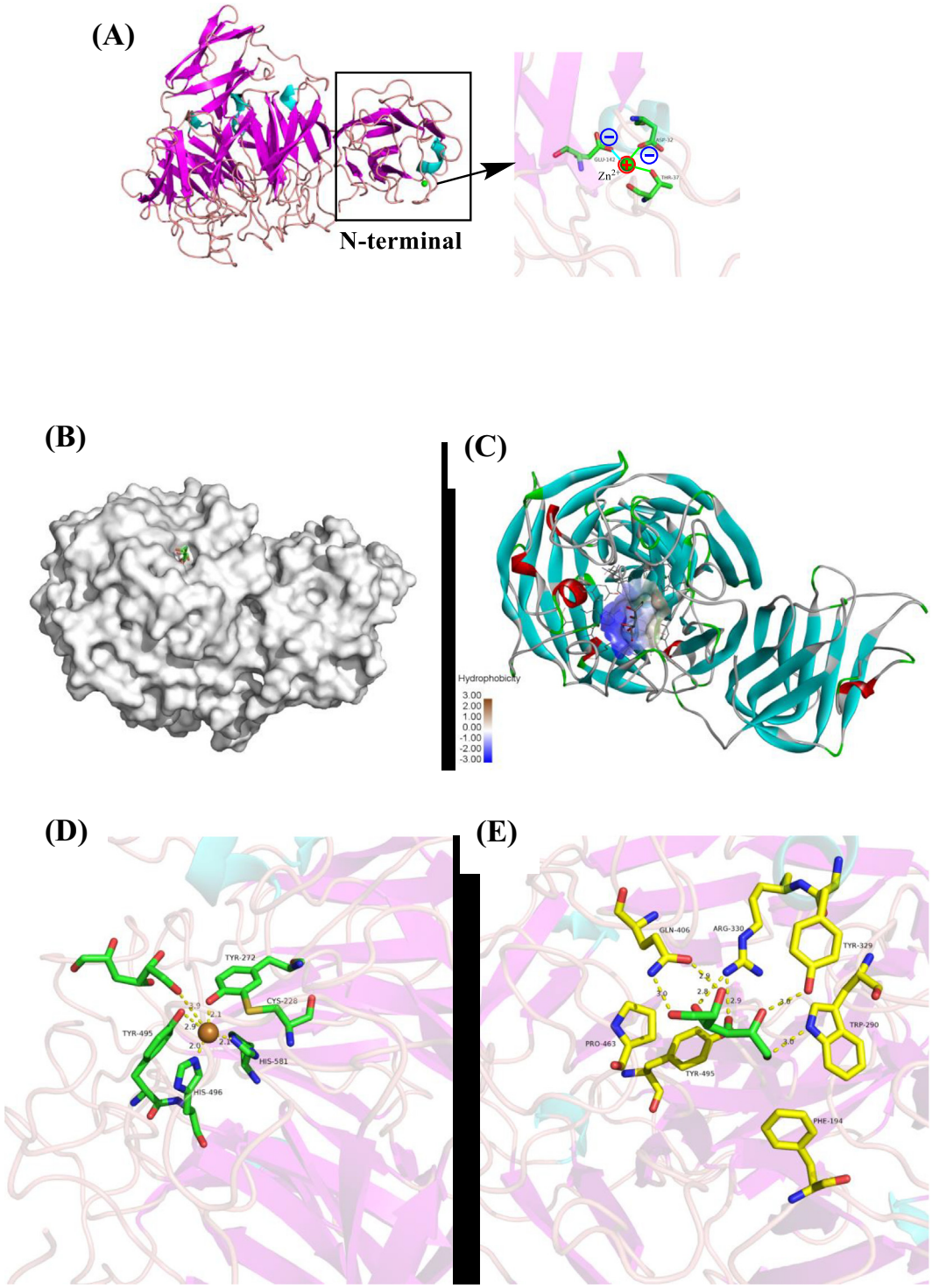

Fig. 6. (A) Docking calculation results between GOX and Zn^{2+}. (B) Overall binding part between GOX and D-Galactose. (C) Specific binding position between GOX and D-Galactose. (D) Catalysis residues of GOX. (E) Interaction residues between GOX catalysis and D-Galactose.

3.6. Selectivity of GOX RTP QDs in D-galactose detection

Some common metal ions and biomolecules in biological liquid are used to study the interference to GOX RTP QDs reaction system (Table S3). When the D-Galactose concentration is 0.1 mM, RTP intensity of the D-Galactose detection system basically remains unchanged by 100 times of K^+, 400 times of Na^+, 12 times of Ca^{2+}, 8 times of Mg^{2+}, 0.0005 times of Fe^{2+}, 0.00001 times of Cu^{2+}, 100 times of glucose, 100 times of saccharose, 40 times of alanine, 0.1 times of proline, 0.1 times of lysine, 0.1 times of glutathione, 0.005 times of cysteine and 0.0006 times of HAS.

3.7. Detection of real samples

To evaluate feasibility of the D-Galactose detection method in actual biological samples, urine was used as the study object (Table S4). The

recovery of spiked sample was between 88%–104%, which indicating that the method is feasible to detect D-Galactose in urine.

4. Conclusions

In this study, a kind of protein GOX functional GOX RTP QDs nano RTP composite was synthesized by using GOX as a template and optimizing the preparation conditions. This GOX RTP QDs not only achieved the protein (enzyme) functional modification of RTP QDs at room temperature, but also improved the catalytic activity of GOX to D-Galactose, and the synthesis method was green and environmental protection. The specific recognition of enzyme and substrate of D-Galactose by GOX and photoinduced electron transfer (PIET) were used to detect the RTP of D-Galactose. Because this method is based on the RTP property of GOX RTP QDs, compared to fluorescent quantum dots, which can avoid the interference of background fluorescence and scattering light, it is particularly suitable for the quantitative detection of D-Galactose in biological samples.

CRediT authorship contribution statement

Jinzhi Lv: Investigation, Formal analysis, Writing - original draft, Writing - review & editing.**Wenli Yang:**Investigation, Data curation. **Yanming Miao:**Investigation, Data curation.

Declaration of competing interest

The authors declare that they have no known competing financial interests or personal relationships that could have appeared to influence the work reported in this paper.

Acknowledgments

The work was completed under the support of the National Natural Science Foundation of China (NSFC) (Grant 31700862).

Appendix A. Supplementary data

Supplementary data to this article can be found online at https://doi.org/10.1016/j.saa.2020.118599.

References

[1] N. Elahi, M. Kamali, M.H. Baghersad, B. Amini, A fluorescence nano-biosensors immobilization on iron (MNPs) and gold (AuNPs) nanoparticles for detection of Shigella spp, Mater. Sci. Eng. C 105 (2019) 110113.
[2] H. Ogi, S. Iwagami, A. Nagakubo, T. Taniguchi, T. Ono, Nano-plate biosensor array using ultrafast heat transport through proteins, Sensors Actuators B: Chemical 278 (2019) 15–20.
[3] M. Dervisevic, M. Alba, B. Prieto-Simon, N.H. Voelcker, Skin in the diagnostics game: wearable biosensor nano- and microsystems for medical diagnostics, Nano Today 30 (2020) 100828.
[4] G. Li, Y. Wu, Y. Li, Y. Hong, X. Zhao, P.I. Reyes, Y. Lu, Early stage detection of Staphylococcus epidermidis biofilm formation using MgZnO dual-gate TFT biosensor, Biosens. Bioelectron. 151 (2020) 111993.
[5] N. Panwar, A.M. Soehartono, K.K. Chan, S. Zeng, G. Xu, J. Qu, et al., Nanocarbons for biology and medicine: sensing, imaging, and drug delivery, Chemical Reviews 119 (2019) 9559–9656.
[6] M. Li, T. Chen, J.J. Gooding, J. Liu, Review of carbon and graphene quantum dots for sensing, ACS Sensors 4 (2019) 1732–1748.
[7] J. Zhang, A. Zhu, T. Zhao, L. Wu, P. Wu, X. Hou, Glucose oxidase-directed, instant synthesis of Mn-doped ZnS quantum dots in neutral media with retained enzymatic activity: mechanistic study and biosensing application, J. Mater. Chem. B 3 (2015) 5942–5950.
[8] P. Wu, T. Zhao, J. Zhang, L. Wu, X. Hou, Analyte-activable probe for protease based on cytochrome C-capped Mn: ZnS quantum dots, Anal. Chem. 86 (2014) 10078–10083.
[9] P. Wu, T. Zhao, Y. Tian, L. Wu, X. Hou, Protein-directed synthesis of Mn-doped ZnS quantum dots: a dual-channel biosensor for two proteins, Chem. Eur. J. 19 (2013) 7473–7479.
[10] L.J. Zhang, L. Xia, H.Y. Xie, Z.L. Zhang, D.W. Pang, Quantum dot based biotracking and biodetection, Anal. Chem. 91 (2019) 532–547.
[11] Y. Miao, X. Sun, J. Lv, G. Yan, Preparation of single-stranded DNA-templated room-temperature phosphorescent quantum dots and their application for mercury(II) detection in environmental and biological fluids, Anal. Chem. 91 (2019) 5036–5042.
[12] Y. Miao, X. Sun, J. Lv, G. Yan, Phosphorescent mesoporous surface imprinting microspheres: preparation and application for transferrin recognition from biological fluids, ACS Appl. Mater. Interfaces 11 (2019) 2264–2272.
[13] Y. Miao, J. Lv, G. Yan, Hybrid detection of target sequence DNA based on phosphorescence resonance energy transfer, Biosens. Bioelectron. 94 (2017) 263–270.
[14] Y. Miao, J. Lv, Y. Li, G. Yan, Construction of biomolecular sensors based on quantum dots, RSC Adv. 6 (2016) 109009–109022.
[15] Y. He, H.-F. Wang, X.-P. Yan, Exploring Mn-doped ZnS quantum dots for the room-temperature phosphorescence detection of enoxacin in biological fluids, Anal. Chem. 80 (2008) 3832–3837.
[16] Y. Miao, M. Yang, G. Yan, Self-assembly of phosphorescent quantum dots/boronic-acid-substituted viologen nanohybrids based on photoinduced electron transfer for glucose detection in aqueous solution, RSC Adv. 6 (2016) 8588–8593.
[17] E. Sotelo-Gonzalez, M.T. Fernandez-Argüelles, J.M. Costa-Fernandez, A. Sanz-Medel, Mn-doped ZnS quantum dots for the determination of acetone by phosphorescence attenuation, Anal. Chim. Acta 712 (2012) 120–126.
[18] P. Wu, J. Zhang, S. Wang, A. Zhu, X. Hou, Sensing during in situ growth of Mn-doped ZnS QDs: a phosphorescent sensor for detection of H_2S in biological samples, Chem. Eur. J. 20 (2014) 952–956.
[19] Y. Miao, Z. Zhang, Y. Gong, Q. Zhang, G. Yan, Self-assembly of manganese doped zinc sulfide quantum dots/CTAB nanohybrids for detection of rutin, Biosens. Bioelectron. 52 (2014) 271–276.
[20] H.-F. Wang, Y.Y. Wu, X.P. Yan, Room-temperature phosphorescent discrimination of catechol from resorcinol and hydroquinone based on sodium tripolyphosphate capped Mn-doped ZnS quantum dots, Anal. Chem. 85 (2013) 1920–1925.
[21] Y. Miao, Z. Zhang, Y. Gong, G. Yan, Phosphorescent quantum dots/doxorubicin nanohybrids based on photoinduced electron transfer for detection of DNA, Biosens. Bioelectron. 59 (2014) 300–306.
[22] Y. Miao, Y. Li, Z. Zhang, G. Yan, Y. Bi, "Turn off–on" phosphorescent biosensors for detection of DNA based on quantum dots/acridine orange, Anal. Chem. 475 (2015) 32–39.
[23] J. Lv, Y. Miao, J. Yang, J. Qin, D. Li, G. Yan, A DNA probe based on phosphorescent resonance energy transfer for detection of transgenic 35S promoter DNA, Biosens. Bioelectron. 91 (2017) 560–565.
[24] L. Cao, J. Zhang, S. Ren, S. Huang, Luminescence enhancement of core-shell ZnS:Mn/ZnS nanoparticles, Appl. Phys. Lett. 80 (2002) 4300–4302.
[25] I. Yildiz, M. Tomasulo, F.M. Raymo, A mechanism to signal receptor-substrate interactions with luminescent quantum dots, Proc. Natl. Acad. Sci. U. S. A. 103 (2006) 11457–11460.
[26] J.H. Chung, C.S. Ah, D.-J. Jang, Formation and distinctive decay times of surface- and lattice-bound Mn2+ impurity luminescence in ZnS nanoparticles, J. Phys. Chem. B 105 (2001) 4128–4132.
[27] R.M. Jones, T.S. Bergstedt, D.W. McBranch, D.G. Whitten, Tuning of Superquenching in layered and mixed fluorescent polyelectrolytes, J. Am. Chem. Soc. 123 (2001) 6726–6727.
[28] C.B. Murphy, Y. Zhang, T. Troxler, V. Ferry, J.J. Martin, W.E. Jones, Probing Förster and Dexter energy-transfer mechanisms in fluorescent conjugated polymer chemosensors, J. Phys. Chem. B 108 (2004) 1537–1543.
[29] M.S. Baptista, G.L. Indig, Effect of BSA binding on photophysical and photochemical properties of triarylmethane dyes, J. Phys. Chem. B 102 (1998) 4678–4688.
[30] H. Lundbck, B. Olsson, Amperometric determination of galactose, lactose and dihydroxyacetone using galactose oxidase in a flow injection system with immobilized enzyme reactors and on-line dialysis, Anal. Lett. 18 (2006) 871–889.
[31] M. Li, J. Yang, Y. Ou, Y. Shi, L. Liu, C. Sun, H. Zheng, Y. Long, Peroxidase-like activity of 2′,7′-difluorofluorescein and its application for galactose detection, Talanta 182 (2018) 422–427.
[32] C.H. Liu, W.L. Tseng, Oxidase-functionalized Fe3O4 nanoparticles for fluorescence sensing of specific substrate, Anal. Chim. Acta 703 (2011) 87–93.
[33] K.N. Lee, Y. Lee, Y. Son, Enhanced sensitivity of a galactose biosensor fabricated with a bundle of conducting polymer microtubules, Electroanalysis 23 (2011) 2125–2130.
[34] P. Wu, Y. He, H.F. Wang, X.P. Yan, Conjugation of glucose oxidase onto Mn-doped ZnS quantum dots for phosphorescent sensing of glucose in biological fluids, Anal. Chem. 82 (2010) 1427–1433.
[35] L. Cao, J. Ye, L. Tong, B. Tang, A new route to the considerable enhancement of glucose oxidase (GOx) activity: the simple assembly of a complex from CdTe quantum dots and GOx, and its glucose sensing, Chem. Eur. J. 14 (2008) 9633–9640.
[36] R. Paukner, P. Staudigl, W. Choosri, D. Haltrich, C. Leitner, Expression, purification, and characterization of galactose oxidase of Fusarium sambucinum in *E. coli*, Protein Expres Purif 108 (2015) 73–79.